

# Structural and electronic properties of Bi<sub>2</sub>Se<sub>3</sub> topological insulator thin films grown by pulsed laser deposition

P. Orgiani, C. Bigi, P. Kumar Das, J. Fujii, R. Ciancio, B. Gobaut, A. Galdi, C. Sacco, L. Maritato, P. Torelli, G. Panaccione, I. Vobornik, and G. Rossi

Citation: *Appl. Phys. Lett.* **110**, 171601 (2017); doi: 10.1063/1.4982207

View online: <https://doi.org/10.1063/1.4982207>

View Table of Contents: <http://aip.scitation.org/toc/apl/110/17>

Published by the [American Institute of Physics](#)

---

## Articles you may be interested in

[Observation of Quantum Hall effect in an ultra-thin \(Bi<sub>0.53</sub>Sb<sub>0.47</sub>\)<sub>2</sub>Te<sub>3</sub> film](#)

*Applied Physics Letters* **110**, 212401 (2017); 10.1063/1.4983684

[Nontrivial surface state transport in Bi<sub>2</sub>Se<sub>3</sub> topological insulator nanoribbons](#)

*Applied Physics Letters* **110**, 053108 (2017); 10.1063/1.4975386

[Detection of current induced spin polarization in epitaxial Bi<sub>2</sub>Te<sub>3</sub> thin film](#)

*Applied Physics Letters* **110**, 122403 (2017); 10.1063/1.4978691

[Emergence of a weak topological insulator from the Bi<sub>x</sub>Se<sub>y</sub> family](#)

*Applied Physics Letters* **110**, 162102 (2017); 10.1063/1.4981875

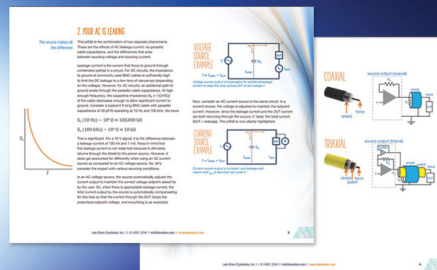
[Cutting a Gordian Knot: Dispersion of plasmonic modes in Bi<sub>2</sub>Se<sub>3</sub> topological insulator](#)

*Applied Physics Letters* **110**, 211601 (2017); 10.1063/1.4984109

[Bi<sub>2</sub>Te<sub>3</sub> photoconductive detectors on Si](#)

*Applied Physics Letters* **110**, 141109 (2017); 10.1063/1.4979839

---



## 5 Electronic Measurement Pitfalls to Avoid

Get the whitepaper

## Structural and electronic properties of Bi<sub>2</sub>Se<sub>3</sub> topological insulator thin films grown by pulsed laser deposition

P. Orgiani,<sup>1,2,a)</sup> C. Bigi,<sup>2,3</sup> P. Kumar Das,<sup>2,4</sup> J. Fujii,<sup>2</sup> R. Ciancio,<sup>2</sup> B. Gobaut,<sup>5</sup> A. Galdi,<sup>1,6</sup> C. Sacco,<sup>1,7</sup> L. Maritato,<sup>1,7</sup> P. Torelli,<sup>2</sup> G. Panaccione,<sup>2</sup> I. Vobornik,<sup>2</sup> and G. Rossi<sup>2,3</sup>

<sup>1</sup>CNR-SPIN, UOS Salerno, 84084 Fisciano, Italy

<sup>2</sup>CNR-IOM, TASC Laboratory in Area Science Park, 34139 Trieste, Italy

<sup>3</sup>Department of Physics, University of Milano, 20133 Milano, Italy

<sup>4</sup>International Centre for Theoretical Physics (ICTP), 34151 Trieste, Italy

<sup>5</sup>Elettra Sincrotrone Trieste, 34139 Trieste, Italy

<sup>6</sup>Department of Information and Electrical Engineering and Applied Mathematics, University of Salerno, 84084 Fisciano, Italy

<sup>7</sup>Department of Industrial Engineering, University of Salerno, 84084 Fisciano, Italy

(Received 20 January 2017; accepted 12 April 2017; published online 24 April 2017)

We report on epitaxial growth of Bi<sub>2</sub>Se<sub>3</sub> topological insulator thin films by Pulsed Laser Deposition (PLD). X-ray diffraction investigation confirms that Bi<sub>2</sub>Se<sub>3</sub> with a single (001)-orientation can be obtained on several substrates in a narrow (i.e., 20 °C) range of deposition temperatures and at high deposition pressure (i.e., 0.1 mbar). However, only films grown on (001)-Al<sub>2</sub>O<sub>3</sub> substrates show an almost-unique in-plane orientation. *In-situ* spin-resolved angular resolved photoemission spectroscopy experiments, performed at the NFFA-APE facility of IOM-CNR and Elettra (Trieste), show a single Dirac cone with the Dirac point at  $E_B \sim 0.38$  eV located in the center of the Brillouin zone and the spin polarization of the topological surface states. These results demonstrate that the topological surface state can be obtained in PLD-grown Bi<sub>2</sub>Se<sub>3</sub> thin films. *Published by AIP Publishing.*  
[\[http://dx.doi.org/10.1063/1.4982207\]](http://dx.doi.org/10.1063/1.4982207)

Over the last decade, topological insulators have attracted great interest for their intriguing conduction mechanisms.<sup>1–3</sup> Even though they are insulating in the bulk, they show a metallic surface state characterized by a unique spin texture, as unambiguously demonstrated by spin-resolved angular resolved photoemission spectroscopy (ARPES) experiments.<sup>4–7</sup> Furthermore, these states are topologically protected against scattering driven by strong spin-orbit interactions, thus being attractive as functional materials for spintronic applications.<sup>8,9</sup> However, for both fundamental studies and electronic applications, high-quality single-crystalline Bi<sub>2</sub>Se<sub>3</sub> thin films, exhibiting topologically protected surface states, are therefore necessary. Moreover, since most of the electronic devices are based on *ad-hoc* tailored multi-layered heterostructures, it is equally necessary to use flexible thin film deposition techniques which would allow the growth of a large variety of functional materials within the same growth system.

In a Pulsed Laser Deposition (PLD) system, the single-atomic species of complex materials are supplied through an ablation process of a target in the form of polycrystalline powders and/or single crystal by the irradiation of a high-intense laser beam. Therefore, multi-layered heterostructures can be easily engineered by positioning the different targets along the laser path, in a continuous vacuum condition. PLD shares with other deposition techniques, such as Molecular Beam Epitaxy (MBE), the high cleanness of the system to prevent any possible contamination and the extremely low deposition rate achievable during the growth (down to 0.01 nm/s). Moreover, since the propagation of the ablated

plume of materials is stopped only at very high pressure (i.e., several mbar), deposition processes at such high partial pressures are indeed possible. Such a capability is particularly important during the growth of materials containing highly volatile atoms (e.g., selenium in the present case), whose re-evaporation rate can be reduced by increasing the background pressure.

We here report on the growth at very high Ar pressure (i.e., 0.1 mbar) of Bi<sub>2</sub>Se<sub>3</sub> thin films. Combining low deposition temperatures ( $\sim 290$  °C) and low deposition rate is the recipe to epitaxially grow Bi<sub>2</sub>Se<sub>3</sub>. We show that the template substrate, while not influencing the bulk structural properties, does have a tremendous impact on the surface structural properties of the films. Highly textured single domain (001)-oriented Bi<sub>2</sub>Se<sub>3</sub> can only be grown on (001) Al<sub>2</sub>O<sub>3</sub> substrates. Our *in-situ* synchrotron radiation x-ray photoemission spectroscopy (XPS), angular resolved photoemission spectroscopy (ARPES) and spin-resolved ARPES data, and *ex-situ* X-ray diffraction (XRD) data prove that we succeeded in growing by PLD high quality Bi<sub>2</sub>Se<sub>3</sub> thin films whose surface hosts the topologically protected surface state with expected helical spin texture.

Bi<sub>2</sub>Se<sub>3</sub> thin films were grown by the PLD technique, at the NFFA-APE facility of IOM-CNR and Elettra in Trieste,<sup>10</sup> using a KrF excimer pulsed laser source ( $\lambda = 248$  nm), with a typical energy density of about 2 J/cm<sup>2</sup>, under a ultra-pure (99.9999%) Ar pressure. Laser pulses were focused on a stoichiometric polycrystalline Bi<sub>2</sub>Se<sub>3</sub> target (purity 99.999%). The typical deposition rate was about 0.07 nm per laser shot and the laser repetition rate was varied from 1 to 10 Hz. Structural properties of thin films were characterized by *in-situ* Low-Energy Electron Diffraction (LEED) and *ex-situ*

<sup>a)</sup>Electronic mail: pasquale.orgiani@spin.cnr.it

XRD, using a four-circle diffractometer with a Cu  $K_\alpha$  radiation source. XPS and ARPES measurements were performed at the APE-NFFA beamline end stations receiving undulator synchrotron radiation from the Elettra storage ring in UHV spectrometer chambers directly connected with the *in-situ* PLD growth apparatus, thus allowing the *in-situ* transferring of the samples.

$\text{Bi}_2\text{Se}_3$  shows a rhombohedral crystal structure (space group  $R\bar{3}m:H$ ) with a periodic stacking of Bi-Se quintuple layers along the out-of-plane  $c$ -axis. The unit cell spans three Bi-Se quintuple layers with lattice constants along the  $a$ -axis and  $c$ -axis of 0.414 nm and 2.864 nm, respectively.<sup>11,12</sup> Remarkably, even though most of the substrates used for the growth have very different in-plane lattice parameters (e.g., (001)  $\text{Al}_2\text{O}_3$ ,<sup>13</sup> (111)  $\text{SrTiO}_3$ ,<sup>14</sup> (001) Si,<sup>15</sup> (111) Si,<sup>16,17</sup> and (111) InP<sup>18</sup>), highly  $c$ -axis oriented  $\text{Bi}_2\text{Se}_3$  thin films have been deposited in all of the cases. However, azimuthal  $\phi$ -scans typically show a six-fold symmetry rather than the expected three-fold one, thus indicating that the film in-plane texturing derives from two domains,  $60^\circ$  rotated with respect to each other.<sup>13,18,19</sup> We here show that such a two-domain in-plane texturing can be substantially removed by using a suitable substrate.

$\text{Bi}_2\text{Se}_3$  thin films were deposited on both (001)  $\text{Al}_2\text{O}_3$  and (111)  $\text{SrTiO}_3$  single crystals. The temperature of the substrate ranged from  $270^\circ\text{C}$  up to  $400^\circ\text{C}$ . After the film growth, the samples were cooled down to room temperature in about 30 min in argon at deposition pressure ranging from  $10^{-5}$  up to  $10^{-1}$  mbar. The growth process at low Ar pressure (i.e., below  $10^{-1}$  mbar) was found to promote Bi segregation, as measured by XPS at the Bi-4f and Se-3d core levels. Similarly, by increasing the growth temperature, Se deficiency is promoted until the  $\text{Bi}_3\text{Se}_4$  phase stabilizes for a growth temperature of about  $330^\circ\text{C}$ . Such a result is not surprising since the  $\text{Bi}_3\text{Se}_4$  shares with the  $\text{Bi}_2\text{Se}_3$  the same rhombohedral crystal structure, with a slightly larger cell length  $a$  of 0.422 nm. However, due to the sizable difference in the  $c$ -axis lattice parameter (i.e., 4.04 nm), the two phases can be discriminated by XRD. A further increase in the temperature turns the film into an amorphous alloy and no diffraction peaks were measured. Best results were obtained for a growth temperature of  $290^\circ\text{C}$  and a low repetition rate of laser pulses (i.e., 1 Hz), under an Ar pressure of  $10^{-1}$  mbar. Interestingly, at such a high deposition pressure, the target-to-substrate distance was crucial in getting the optimal Se:Bi chemical ratio. The optimal target-to-substrate distance, in our geometry, was found to be 48 mm. As a matter of fact, like other complex systems,<sup>20</sup> as the background pressure increases, the films are deposited from a progressively more confined ablation plume. This might selectively affect both the energy and the efficiency of the single-species transferring to the growing film. This is what is likely happening also in the case of  $\text{Bi}_2\text{Se}_3$  deposition, where heavy (i.e., Bi) and light (i.e., Se) elements can be stopped at different target-to-substrate distances, therefore determining slight changes in the Bi:Se chemical ratio (e.g., samples deposited at a distance of 50 mm are slightly Se deficient).

XRD symmetrical  $\theta$ - $2\theta$  scans of optimized  $\text{Bi}_2\text{Se}_3$  thin films only contain (00l) peaks, indicating the preferential  $c$ -axis orientation of the film along the [001]  $\text{Al}_2\text{O}_3$  and the [111]  $\text{SrTiO}_3$  substrates' crystallographic directions (Fig. 1).

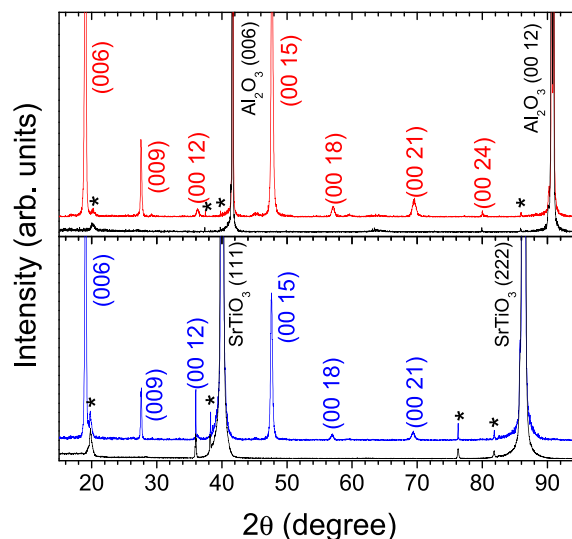


FIG. 1. Symmetrical  $\theta$ - $2\theta$  scan of a  $\text{Bi}_2\text{Se}_3$  thin film grown on a (001)- $\text{Al}_2\text{O}_3$  (red curve in upper panel) and  $\text{SrTiO}_3$  (blue curve in lower panel) substrates. For reference, the spectra of bare (001)- $\text{Al}_2\text{O}_3$  and (111)- $\text{SrTiO}_3$  substrates are also reported as black curves (asterisks indicate spurious peaks recorded using a diffractometer on both films and bare substrates).

By symmetric (00 15) Bragg reflections, the out-of-plane  $c$ -axis parameters were found to be 2.861 nm and 2.862 nm for films grown on  $\text{Al}_2\text{O}_3$  and  $\text{SrTiO}_3$  substrates, respectively, thus indicating a substantial structurally relaxed growth on those substrates. The azimuthal  $\phi$ -scan of  $\text{Bi}_2\text{Se}_3$  thin films grown on  $\text{Al}_2\text{O}_3$  (panel (a) of Fig. 2) shows a substantial three-fold symmetry of the film which epitaxially grows on C-sapphire with a  $60^\circ$  in-plane rotation of the unit cell with respect to the substrate. The very low intensity of the second series of diffraction peaks at  $60^\circ$  from the major peaks indicates that the double-domain structure is strongly suppressed. However, even though showing the same  $c$ -axis preferential orientation,  $\text{Bi}_2\text{Se}_3$  thin films grown on the (111)  $\text{SrTiO}_3$  substrate were not well ordered in the surface plane. In the azimuthal  $\phi$ -scan (panel (b) of Fig. 2), the second series of diffraction peaks is more intense than that reported for the film grown on (001)  $\text{Al}_2\text{O}_3$  and the background signal is not-zero, thus indicating a fraction of in-plane randomly oriented  $\text{Bi}_2\text{Se}_3$  domains.

Since XRD is a bulk sensitive technique, the surface order of the PLD grown films was also checked by LEED. In full agreement with the bulk sensitive XRD analyses, the LEED pattern of *in-situ* transferred  $\text{Bi}_2\text{Se}_3$  thin films grown on  $\text{Al}_2\text{O}_3$  (panel (c) of Fig. 2) shows sharp diffraction spots exhibiting the expected three-fold symmetry, thus confirming the  $\text{Bi}_2\text{Se}_3$  triangular in-plane symmetry. However, films grown on the  $\text{SrTiO}_3$  (panel (d) of Fig. 2) show broad diffraction spots exhibiting a six-fold symmetry with a continuous connecting ring, indicating the presence of a randomly in-plane distributed disordered phase. In the case of  $\text{Bi}_2\text{Se}_3$  thin films grown on  $\text{SrTiO}_3$  substrates, the surface structural/electronic properties can be very unsuitable for device applications and/or advanced probing techniques (e.g., spin-resolved ARPES experiments on mis-oriented grains lead to very broad spectral features or even no detectable band dispersion). On the contrary,  $\text{Bi}_2\text{Se}_3$  thin films grown on (001)  $\text{Al}_2\text{O}_3$  show an almost unique in-plane structural arrangement, thus making them ideal candidates in the cited cases.

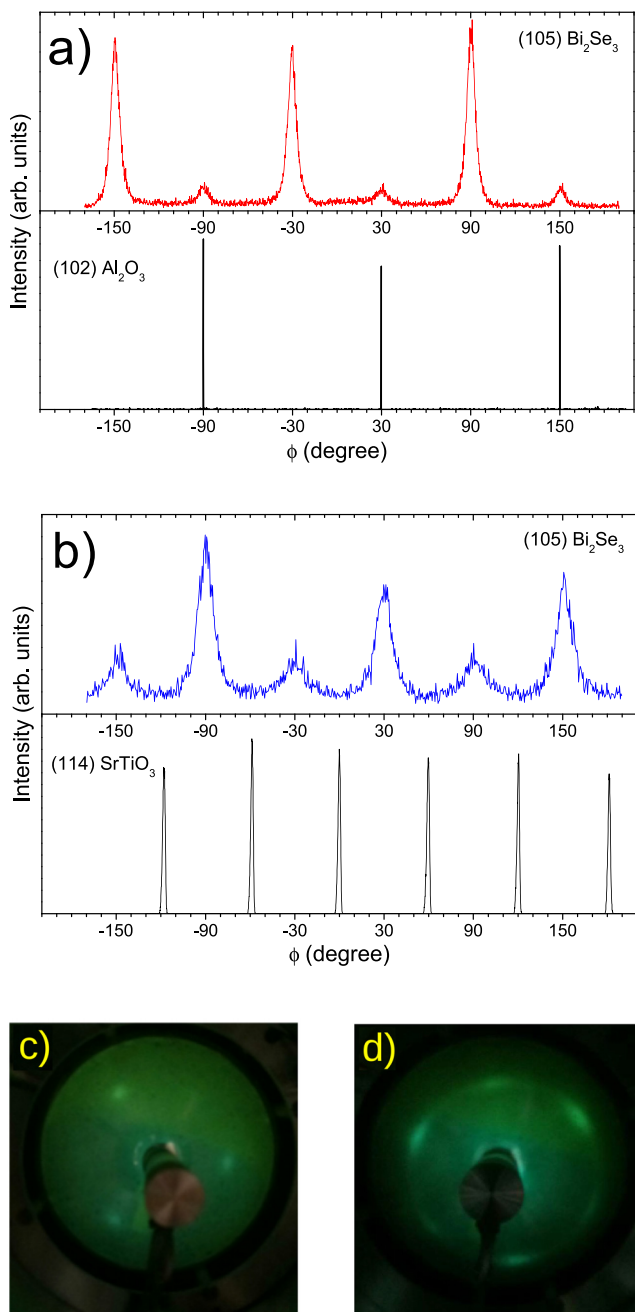


FIG. 2. Azimuthal  $\phi$ -scans around the (105)  $\text{Bi}_2\text{Se}_3$  asymmetric reflections for  $\text{Bi}_2\text{Se}_3$  films grown on  $\text{Al}_2\text{O}_3$  (panel (a)) and  $\text{SrTiO}_3$  (panel (b)) substrates, respectively; as reference, azimuthal  $\phi$ -scans around the (102)  $\text{Al}_2\text{O}_3$  and (114)  $\text{SrTiO}_3$  asymmetric reflections are also reported as black curves in the panels; (c) and (d) LEED patterns of  $\text{Bi}_2\text{Se}_3$  thin films grown on  $\text{Al}_2\text{O}_3$  and  $\text{SrTiO}_3$  substrates, respectively.

The electronic properties and the chemical composition of  $\text{Bi}_2\text{Se}_3$  thin films were explored by measuring core level photoemission spectra. The XPS survey scan displays main peaks of both Bi and Se<sup>21–23</sup> with no trace of either Bi<sup>24</sup> or Se<sup>25</sup> segregation. In the case of pure Bi clusters, the 4f final states would show at 162.3 eV/157.0 eV binding energy (panel (a) of Fig. 3); for Se aggregates, the binding would be at 55.1/55.3 eV with 0.86 eV spin-orbit splitting, well separated with respect to the observed peaks belonging to  $\text{Bi}_2\text{Se}_3$  (panel (b) in Fig. 3). Details of the relevant core level peaks are presented in the panels of Fig. 3, with the results of fitting routines to elucidate the lineshapes and energy separation. In

panel (a), the Bi 4f–Se 3p core lines show Se-related peaks shifting by 2.5 eV towards lower binding energies while Bi-peaks to higher binding energies (i.e.,  $\Delta E = 0.7$  eV), with respect to pure elemental aggregates. Such a behavior, attributed to the net charge flow with hybridized bonds between Bi and Se, is also observed on other Bi chalcogenide systems.<sup>13</sup>

Because of the large (i.e., 10%) experimental indetermination of the chemical composition from present XPS data due to possible errors in the fitting routine and background subtraction and the presence of photoelectron diffraction effects, as already reported in crystalline topological insulators,<sup>26,27</sup> we performed energy dispersive spectroscopy (EDS) analysis, which is capable of an improved resolution in determining the chemical composition (i.e., experimental error of about 5%). The Bi:Se chemical ratio was found to be 1.5, thus indicating a correct stoichiometry of the  $\text{Bi}_2\text{Se}_3$  thin films. Interestingly, even in the case of a slight Se-deficiency (for instance tuned by varying the target-to-substrate distance, as previously discussed), the topological properties (i.e., a single Dirac cone with well-defined spin-texturing) are not lost, while the Dirac cone is rigidly shifted to higher binding energies as already reported for thin films<sup>4,6</sup> and also for single crystals.<sup>28–30</sup>

Spin and angular resolved photoemission experiments were performed on *in-situ* transferred as-grown  $\text{Bi}_2\text{Se}_3$  thin films at a temperature of 77 K and with a synchrotron radiation spot of about  $100 \times 50 \mu\text{m}$ . In order to better resolve the topological surface states features, ARPES investigation was performed at a suitable photon energy ( $h\nu = 55$  eV) that strongly reduces the photoemission intensity from the bulk conduction band. ARPES data of a  $\text{Bi}_2\text{Se}_3$  thin film grown on  $\text{Al}_2\text{O}_3$  are shown in Fig. 4.

The ARPES features (panels (a), (b), and (c) of Fig. 4) are in good agreement with the ones measured on cleaved single crystals<sup>28</sup> and thin films grown by MBE.<sup>7</sup> As a matter of fact, the characteristic signature of the topological surface state can be easily observed: two linearly dispersing metallic states cross the Fermi level at  $k_{\parallel} \sim \pm 0.1 \text{ \AA}^{-1}$  and the two branches intersecting at  $\Gamma$ . The position of the Dirac point was determined by looking at the width of several Momentum Distribution Curves (MDCs) of the ARPES spectrum and comparing the FWHMs. The Dirac point was estimated to be at  $E_B = 0.38 \pm 0.03$  eV binding energy, which is slightly larger than the expected value of 300 meV obtained by calculations.<sup>3</sup> It is worth noticing that such a discrepancy frequently occurs in  $\text{Bi}_2\text{Se}_3$  thin films<sup>13,14</sup> and also in single crystals.<sup>2,7,31</sup> Such a result indicates the slight presence of Se vacancies, probably near the surface, which act as electron donor sites in the  $\text{Bi}_2\text{Se}_3$  compound, populating the conduction band and shifting rigidly the band structure towards higher binding energies (e.g., for a Se:Bi ratio of about 1.38, the Dirac point has been measured at about 0.6 eV). However, charge carrier density can be tuned by partially replacing Bi atoms with a very small amount ( $\sim 0.6\%$ ) of divalent ions (e.g.,  $\text{Ca}^{2+}$ ), thus having the bulk insulating behavior restored.<sup>31</sup>

The spin texture of the Dirac cone was mapped by using a very-low energy electron diffraction (VLEED) based vectorial spin polarimeter recently developed at the APE-NFFA beamline.<sup>32</sup> Spin-resolved results, obtained along the quantization axis laying in the sample surface plane perpendicular

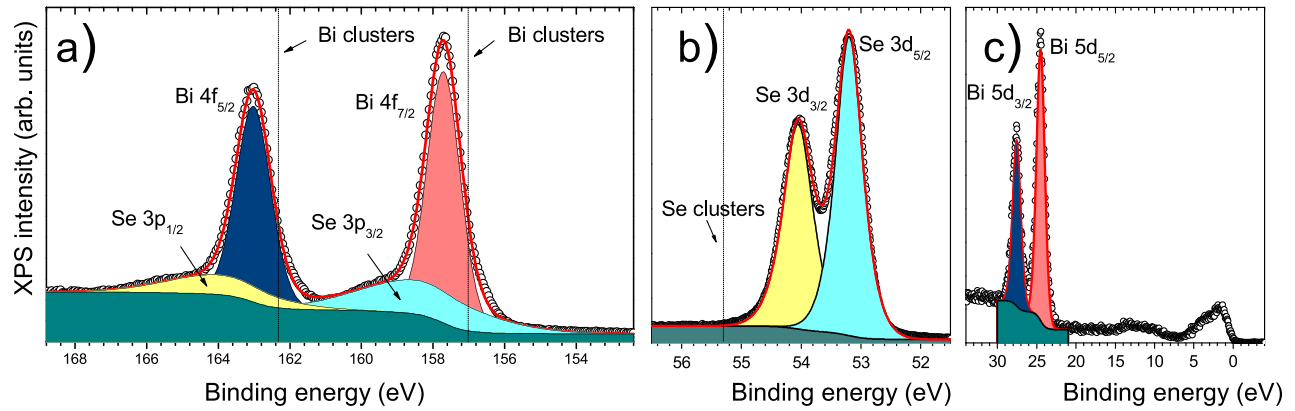


FIG. 3. High-resolution XPS scans of Se-3p/Bi-4f peaks (panel (a)), Se-3d peaks (panel (b)), and Bi-5d peaks along with the valence band (panel (c)); excitation photon energy is 920 eV. Results of fitting procedures are also reported; expected binding energies for both Bi and Se segregation are also reported in panels (a) and (b), respectively.

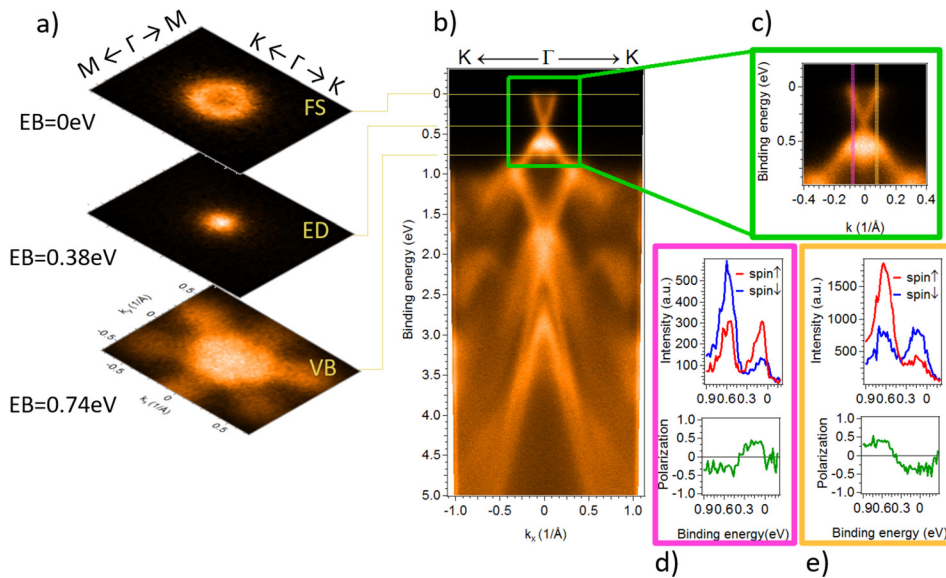


FIG. 4. Spin-ARPES data of the topological surface state of a  $\text{Bi}_2\text{Se}_3$  thin film: (a) Constant energy contours at 0 eV ( $E_F$ ), 0.38 eV ( $E_D$ ), and 0.74 eV, respectively; (b) valence band along the  $\text{K}-\Gamma-\text{K}$  high symmetry axis (photon energy is  $h\nu = 55$  eV); (c) zooming out of the topological surface state; (d)–(e) spin-resolved curves and the corresponding spin polarization showing the spin texture of the Dirac cone extracted at  $k_{\parallel} = \pm 0.08 \text{ \AA}^{-1}$ .

to the crystalline momentum, are reported in panels (d) and (e) of Fig. 4, where the spin-resolved curves and the spin polarization deduced from the Energy Distribution Curves (EDCs) measured at  $k_{\parallel} = \pm 0.08 \text{ \AA}^{-1}$  in the  $k$ -space are shown. In particular, data confirm the expected helical spin texture of the topological insulators: namely, two linear branches of the Dirac cone spin polarized characterized by opposite spin polarization for positive and negative momenta. Furthermore, as expected, the spin chirality reverses above and below the Dirac point. From the spin polarization analysis, the estimated polarization value is  $\sim \pm 40\%$ , lower than the expected 100%. However, such a feature is quite common, even in the case of single crystals, and it has been discussed thoroughly from both the theoretical and experimental point of view.<sup>33–35</sup> Nevertheless, from the whole set of both ARPES and spin-ARPES results, it can be concluded that the PLD-grown  $\text{Bi}_2\text{Se}_3$  thin films do show metallic surface states that evidence the spin features fingerprints of the topological insulators.

In conclusion, we have shown that high quality epitaxial  $\text{Bi}_2\text{Se}_3$  thin films can be grown by Pulsed Laser Deposition. The combination of low deposition temperature (i.e., 290 °C), high deposition pressure (i.e., 0.1 mbar), and low deposition

rate (i.e., 1 Hz) is crucial to obtain well ordered  $\text{Bi}_2\text{Se}_3$  epitaxial thin films. Moreover, the use of the (001)  $\text{Al}_2\text{O}_3$  substrate provides an almost-unique structural texturing of the  $\text{Bi}_2\text{Se}_3$  thin films. Spin-resolved ARPES data exhibit a single Dirac cone with a well-defined spin polarization texture of the topological surface states. Moreover, even in the presence of a slight Se deficiency, the topological surface states are protected and the Dirac cone is rigidly shifted towards higher binding energies. Such a feature opens perspectives in emerging spintronic planar devices based on multi-layered heterostructures technology in which one functional layer is the topological insulator  $\text{Bi}_2\text{Se}_3$ .

This work has been performed in the framework of the Nanoscience Foundry and Fine Analysis (NFFA-MIUR Italy Progetti Internazionali) facility. This work has been supported by NOXSS PRIN (2012Z3N9R9) Project of MIUR, Italy.

<sup>1</sup>L. Fu, C. L. Kane, and E. J. Mele, *Phys. Rev. Lett.* **98**, 106803 (2007).

<sup>2</sup>Y. Xia, D. Qian, D. Hsieh, L. Wray, A. Pal, H. Lin, A. Bansil, D. Grauer, Y. S. Hor, R. J. Cava, and M. Z. Hasan, *Nat. Phys.* **5**, 398 (2009).

<sup>3</sup>H. Zhang, C.-X. Liu, X.-L. Qi, X. Dai, Z. Fang, and S.-C. Zhang, *Nat. Phys.* **5**, 438 (2009).

- <sup>4</sup>S.-Y. Xu, M. Neupane, C. Liu, D. Zhang, A. Richardella, L. A. Wray, N. Alidoust, M. Leandersson, T. Balasubramanian, J. Sanchez-Barriga, O. Rader, G. Landolt, B. Slomski, J. H. Dil, J. Osterwalder, T.-R. Chang, H.-T. Jeng, H. Lin, A. Bansil, N. Samarth, and M. Z. Hasan, *Nat. Phys.* **8**, 616 (2012).
- <sup>5</sup>D. Zhang, A. Richardella, D. W. Rench, S.-Y. Xu, A. Kandala, T. C. Flanagan, H. Beidenkopf, A. L. Yeats, B. B. Buckley, P. V. Klimov, D. D. Awschalom, A. Yazdani, P. Schiffer, M. Z. Hasan, and N. Samarth, *Phys. Rev. B* **86**, 205127 (2012).
- <sup>6</sup>H. M. do Nascimento Vasconcelos, M. Eddrief, Y. Zheng, D. Demaille, S. Hidki, E. Fonda, A. Novikova, J. Fujii, P. Torelli, B. Rache Salles, I. Vobornik, G. Panaccione, A. J. Aparecido de Oliveira, M. Marangolo, and F. Vidal, *ACS Nano* **10**, 1132 (2016).
- <sup>7</sup>F. Vidal, M. Eddrief, B. Rache Salles, I. Vobornik, E. Velez-Fort, G. Panaccione, and M. Marangolo, *Phys. Rev. B* **88**, 241410(R) (2013).
- <sup>8</sup>R. Mellnik, J. S. Lee, A. Richardella, J. L. Grab, P. J. Mintun, M. H. Fischer, A. Vaezi, A. Manchon, E.-A. Kim, N. Samarth, and D. C. Ralph, *Nature* **511**, 449 (2014).
- <sup>9</sup>Y. Kubota, K. Murata, J. Miyawaki, K. Ozawa, M. C. Onbasli, T. Shirasawa, B. Feng, S. Yamamoto, R.-Y. Liu, S. Yamamoto, S. K. Mahatha, P. Sheverdyayeva, P. Moras, C. A. Ross, S. Suga, Y. Harada, K. L. Wang, and I. Matsuda, *J. Phys. Condens. Matter* **29**, 055002 (2017).
- <sup>10</sup>See <http://www.trieste.nffa.eu> for more information about the NFFA-APE facility.
- <sup>11</sup>H. Lind, S. Lidin, and U. Haussermann, *Phys. Rev. B* **72**, 184101 (2005).
- <sup>12</sup>H. Okamoto, *J. Phase Equilib.* **15**, 195 (1994).
- <sup>13</sup>Y. F. Lee, S. Punugupati, F. Wu, Z. Jin, J. Narayan, and J. Schwartz, *Curr. Opin. Solid State Mater. Sci.* **18**, 279 (2014).
- <sup>14</sup>P. H. Le, K. H. Wu, C. W. Luo, and J. Leu, *Thin Solid Films* **534**, 659 (2013).
- <sup>15</sup>L. Meng, H. Meng, W. Gong, W. Liu, and Z. Zhang, *Thin Solid Films* **519**, 7627 (2011).
- <sup>16</sup>G. Zhang, H. Qin, J. Teng, J. Guo, Q. Guo, X. Dai, Z. Fang, and K. Wu, *Appl. Phys. Lett.* **95**, 053114 (2009).
- <sup>17</sup>P. H. Le, C.-N. Liao, C. W. Luo, J.-Y. Lin, and J. Leu, *Appl. Surf. Sci.* **285P**, 657 (2013).
- <sup>18</sup>S. Schreyeck, N. V. Tarakina, G. Karczewski, C. Schumacher, T. Borzenko, C. Brüne, H. Buhmann, C. Gould, K. Brunner, and L. W. Molenkamp, *Appl. Phys. Lett.* **102**, 041914 (2013).
- <sup>19</sup>Y. F. Lee, R. Kumar, F. Hunte, J. Narayan, and J. Schwartz, *J. Appl. Phys.* **118**, 125309 (2015).
- <sup>20</sup>P. Orgiani, R. Ciancio, A. Galdi, S. Amoruso, and L. Maritato, *Appl. Phys. Lett.* **96**, 032501 (2010).
- <sup>21</sup>J. A. Bearden and A. F. Burr, *Rev. Mod. Phys.* **39**, 125 (1967).
- <sup>22</sup>M. Cardona and L. Ley, *Photoemission in Solids I: General Principles* (Springer-Verlag, Berlin, Germany, 1978).
- <sup>23</sup>J. C. Fuggle and N. Mårtensson, *J. Electron Spectrosc. Relat. Phenom.* **21**, 275 (1980).
- <sup>24</sup>A. S. Hewitt, J. Wang, J. Boltersdorf, P. A. Muggard, and D. B. Dougherty, *J. Vac. Sci. Technol. B* **32**, 04E103 (2014).
- <sup>25</sup>Y.-C. Yeh, P.-H. Ho, C.-Y. Wen, G.-J. Shu, R. Sankar, F.-C. Chou, and C.-W. Che, *J. Phys. Chem. C* **120**, 3314 (2016).
- <sup>26</sup>K. Kuroda, M. Ye, E. F. Schwier, M. Nurmamat, K. Shirai, M. Nakatake, S. Ueda, K. Miyamoto, T. Okuda, H. Namatame, M. Taniguchi, Y. Ueda, and A. Kimura, *Phys. Rev. B* **88**, 245308 (2013).
- <sup>27</sup>M. V. Kuznetsov, L. V. Yashina, J. Sanchez-Barriga, I. I. Ogorodnikov, A. S. Vorokh, A. A. Volykhov, R. J. Koch, V. S. Neudachina, M. E. Tamm, A. P. Sirotnina, A. Y. Varykhalov, G. Springholz, G. Bauer, J. D. Riley, and O. Rader, *Phys. Rev. B* **91**, 085402 (2015).
- <sup>28</sup>J. G. Analytis, J.-H. Chu, Y. Chen, F. Corredor, R. D. McDonald, Z. X. Shen, and I. R. Fisher, *Phys. Rev. B* **81**, 205407 (2010).
- <sup>29</sup>D. Hsieh, Y. Xia, D. Qian, L. Wray, J. H. Dil, F. Meier, J. Osterwalder, L. Patthey, J. G. Checkelsky, N. P. Ong, A. V. Fedorov, H. Lin, A. Bansil, D. Grauer, Y. S. Hor, R. J. Cava, and M. Z. Hasan, *Nature* **460**, 1101 (2009).
- <sup>30</sup>O. Chiatti, C. Riha, D. Lawrenz, M. Busch, S. Dusari, J. Sánchez-Barriga, A. Mogilatenko, L. V. Yashina, S. Valencia, A. A. Ünal, O. Rader, and S. F. Fischer, *Scientific Reports* **6**, 27483 (2016).
- <sup>31</sup>Z. Wang, T. Lin, P. Wei, X. Liu, R. Dumas, K. Liu, and J. Shi, *Appl. Phys. Lett.* **97**, 042112 (2010).
- <sup>32</sup>C. Bigi, J. Fujii, I. Vobornik, P. K. Das, D. Benedetti, F. Salvador, G. Panaccione, and G. Rossi, e-print [arXiv:1610.06922](https://arxiv.org/abs/1610.06922) [physics.ins-det].
- <sup>33</sup>O. V. Yazyev, J. E. Moore, and S. G. Louie, *Phys. Rev. Lett.* **105**, 266806 (2010).
- <sup>34</sup>Z.-H. Zhu, C. N. Veenstra, S. Zhdanovich, M. P. Schneider, T. Okuda, K. Miyamoto, S.-Y. Zhu, H. Namatame, M. Taniguchi, M. W. Haverkort, I. S. Elfimov, and A. Damascelli, *Phys. Rev. Lett.* **112**, 076802 (2014).
- <sup>35</sup>G. Landolt, S. Schreyeck, S. V. Ereemeev, B. Slomski, S. Muff, J. Osterwalder, E. V. Chulkov, C. Gould, G. Karczewski, K. Brunner, H. Buhmann, L. W. Molenkamp, and J. H. Dil, *Phys. Rev. Lett.* **112**, 057601 (2014).